

A NEW FAMILY OF ROBUST NON GAUSSIAN DETECTORS BASED ON A GEOMETRIC HEURISTIC

Olivier Rabaste and Nicolas Trouvé

ONERA, the French Aerospace Lab, DEMR/TSI
Chemin de la Hunière 91761 Palaiseau Cedex, France
Email: {firstname.lastname}@onera.fr

ABSTRACT

This paper addresses the detection problem in moderately non-Gaussian environments. We first propose an analysis of the classical Gaussian and SIRV detectors from a new point of view. We define a robustness criteria with respect to signal mismatch and we demonstrate that the non-Gaussian detector is robust only for small mismatches. We then propose a new family of detectors based on a geometric heuristic that exploits advantages of both Gaussian and non-Gaussian detectors. This new family is robust to signal mismatch and presents very interesting detection performance.

1. INTRODUCTION

With the unceasing improvement in the measurement technologies, more and more radar applications must cope with non-Gaussian clutter [3]. For instance, non-Gaussian noise usually arises in SAR imaging as higher resolutions are reached. Difficult measurement conditions such as severe weather in the case of sea measurements, or low grazing angle can also lead to impulsive distributions. Gaussian models are then not adapted. When the clutter statistic is well documented, specific statistical models may be employed instead; for instance ground or sea clutter may be modelled with a K-distribution or a Weibull distribution [1, 2]. However, when the clutter distribution is unknown, or difficult to model, more general clutter models must be considered. Unfortunately these more general models are less performant in moderately impulsive noise. This problem arises in nowadays radar applications. Indeed, as the resolution improves, the clutter statistic continuously evolves from Gaussian to more impulsive distributions. Desired detectors should be able to handle a large variety of clutter distribution from Gaussian to moderately non-Gaussian clutter.

Among the clutter models, Spherically Invariant Random Vectors (SIRV) [10] are very promising, since they can model a wide range of random processes. When injected in the classical hypothesis testing problem, this model leads to a new detector, the GLRT-LQ (GLRT-Linear Quadratic) detector [3], derived in the Generalized Likelihood Ratio Test (GLRT) framework to deal with an unknown amplitude. Interestingly this detector has also been obtained under different hypotheses: it corresponds to the Normalized Matched Filter (NMF) derived in [9] for a Gaussian noise with unknown level, or to the asymptotic Bayesian Optimum Radar Detector (BORD) obtained from a Bayesian perspective in [6]. For unicity, we will refer to it in this article as the GLRT-SIRV detector, while we will denote by GLRT-GAUSS the classical Gaussian detector with unknown amplitude. Both GLRT-GAUSS and GLRT-SIRV detectors are obtained in the GLRT framework that is only a heuristic procedure to

design detectors for composite hypothesis testing problems, and they are therefore optimal only in their respective classes of invariance.

Both detectors have quite different behaviors, that can be characterized by the geometry of their respective acceptance regions. This was first done in [9]. In this article, we propose to move one step further and exploit the specificities of these geometries, first to highlight some interesting characteristics of the two detectors, and second to design a new family of detectors that gathers advantages of both detectors.

The GLRT-SIRV detector is very efficient in heterogeneous or non stationary environment. But it presents also some drawbacks seldom discussed in the literature. Contrary to the GLRT-GAUSS detector, the GLRT-SIRV detector is intrinsically multidimensional: the signal considered must be a vector of dimension at least 2. It is then dependent to the dimension; we will see in this article that the performance of the GLRT-SIRV is highly dependent to this parameter. Another feature of importance is the reliability of the detector when the steering vector is not perfectly known; this may arise in any scenario when the backscattering signal is difficult to model, for example when it is sensitive to target orientation, propagation errors, angular or frequency dependence. Solutions for signal mismatch have been proposed in [5, 4] assuming that the useful signal lies within a conic region.

Here we use a different approach based on the detector geometry: we first demonstrate the impact of dimension and mismatch on the GLRT-GAUSS and GLRT-SIRV detection performance; in particular we provide new results concerning their robustness to signal mismatch. It is then of interest to design new detectors sharing good characteristics of both GLRT-GAUSS and GLRT-SIRV. While this was the objective of the ASB (Adaptive Sidelobe Blanker) [8], this detector was not defined from a geometry perspective and is not robust for all mismatches. The second contribution of this paper is then the design of a new family of detectors based on a geometric heuristic that takes advantage of both GLRT-GAUSS and GLRT-SIRV interesting properties; in particular, we demonstrate the robustness of the proposed detectors.

This paper is organized as follows: in section 2, we present the GLRT-GAUSS and GLRT-SIRV, and study their behavior with respect to dimension and signal mismatch. Then in section 3, we describe the new family of detectors.

2. GLRT-GAUSS AND GLRT-SIRV STUDY

2.1 GLRT-GAUSS and GLRT-SIRV detectors

In this section we present the GLRT-GAUSS and GLRT-SIRV detectors. The detection problem in SIRV clutter can be written as the following hypothesis testing problem:

$$\begin{cases} \mathcal{H}_0 : \mathbf{y} = \mathbf{n} & \text{(noise only),} \\ \mathcal{H}_1 : \mathbf{y} = \mathbf{A}s + \mathbf{n} & \text{(signal + noise),} \end{cases} \quad (1)$$

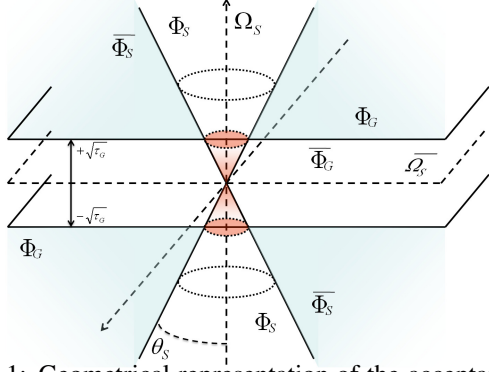


Figure 1: Geometrical representation of the acceptance and rejection regions of the GLRT-GAUSS and GLRT-SIRV.

with \mathbf{y} the received signal, \mathbf{s} the transmitted signal or the steering vector of dimension m , A the unknown complex amplitude and \mathbf{n} a SIRV noise. \mathbf{n} can be written as $\mathbf{n} = \sqrt{\kappa}\mathbf{x}$, where κ is the texture, i.e. a positive random variable of unknown probability density function (pdf), and \mathbf{x} is a complex zero-mean Gaussian vector with covariance matrix Γ [10].

The GLRT-GAUSS detector is the GLRT solution to problem (1) when the noise is Gaussian and the amplitude unknown. It corresponds to the test statistic:

$$\mathcal{T}_G = \frac{|\mathbf{s}^H \Gamma^{-1} \mathbf{y}|^2}{\|\mathbf{s}\|_{\Gamma^{-1}}^2} \underset{\mathcal{H}_0}{\overset{\mathcal{H}_1}{\gtrless}} \tau_G, \quad (2)$$

where \mathbf{x}^H denotes the hermitian transpose of vector \mathbf{x} and $\|\mathbf{x}\|_{\Gamma^{-1}}^2 = \mathbf{x}^H \Gamma^{-1} \mathbf{x}$ is the norm associated to the inner product induced by Γ^{-1} . Geometrically, this detector resorts to projecting the received signal \mathbf{y} onto the signal subspace Ω_S of the vector space \mathbb{C}^m and accepting all resulting vectors with sufficiently large norm. The detector threshold can then be represented by two hyperplanes in \mathbb{C}^m . Acceptance and rejection region Φ_G and $\overline{\Phi}_G$ are depicted in Fig.1.

The GLRT-SIRV detector can be viewed as a GLRT solution to the hypothesis testing problem (1) for a SIRV noise when both the amplitude and the SIRV texture are unknown, deterministic, and replaced by their respective Maximum Likelihood estimates. It corresponds to the test statistic:

$$\mathcal{T}_S = \frac{|\mathbf{s}^H \Gamma^{-1} \mathbf{y}|^2}{\|\mathbf{s}\|_{\Gamma^{-1}}^2 \|\mathbf{y}\|_{\Gamma^{-1}}^2} \underset{\mathcal{H}_0}{\overset{\mathcal{H}_1}{\gtrless}} \tau_S. \quad (3)$$

Thanks to Cauchy-Schwarz inequality, we can write $\mathcal{T}_S = \cos^2 \theta_S$; the angle θ_S can be defined even in the complex case. Then the GLRT-SIRV consists in projecting the received signal onto the unit sphere and accepting signals contained in a spherical cap centered on Ω_S and defined by angle θ_S . In other words, the GLRT-SIRV resorts to accepting any signal \mathbf{y} falling into a double cone of axis Ω_S and angle θ_S . Acceptance and rejection region Φ_S and $\overline{\Phi}_S$ are plotted in Fig.1.

Finally, note that throughout this paper, we consider the SNR at the output of the matched filter, defined by $\rho = |A|^2 \|\mathbf{s}\|_{\Gamma^{-1}}^2 / \|\mathbf{n}\|_{\Gamma^{-1}}^2$. This definition takes into account the energy of the transmitted signal or compression gain.

2.2 Effect of signal dimension

The effect of the dimension can be studied on the expressions of the detection threshold and the false alarm probability P_{FA} . For the GLRT-GAUSS detector, the relationship, provided in the complex case by $P_{FA} = \exp(-\sqrt{\tau_G})$ (see [7]), is independent from the dimension parameter m : for a given false alarm probability, the detection threshold is the same whatever the

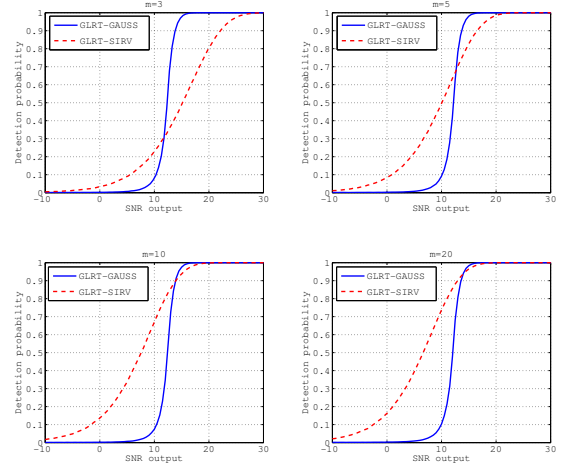


Figure 2: Detection performance for different dimensions for the GLRT-GAUSS and GLRT-SIRV in a K-distributed noise with shape parameter $\nu = 1$; $P_{FA} = 10^{-3}$.

dimension, and, since we consider the output SNR, detection performance of the GLRT-GAUSS are invariant with the dimension. On the contrary, since the false alarm probability for the GLRT-SIRV is given by $P_{FA} = (1 - \tau_S)^{m-1}$ (see [3]), the detection threshold (or detection angle) must be changed according to the dimension to ensure the same P_{FA} .

This phenomenon can be geometrically explained: as the SIRV noise is spherically invariant, the false alarm probability is simply provided by the ratio between the surface of a spherical cap defined by angle θ and the surface of the unit sphere. For a given angle, this ratio decreases when increasing the dimension since the surface outside the spherical cap is more inflated than the surface inside (this is true for any angle lower than $\pi/2$). So the detection angle increases with the dimension to ensure a fixed P_{FA} , thus widening the cone aperture, and increasing the distance between the noiseless signal $A\mathbf{s}$ and the detection cone. Since the detection probability P_D greatly depends on this distance, the increase in the detection angle leads to better detection performance for larger dimensions. This is verified on simulation in Fig.2.

Finally, we notice in Fig.2 that the GLRT-SIRV presents worse detection performance at high SNR than the GLRT-GAUSS, even in SIRV noise. Although this may seem surprising at first sight, it does not contradict the theory, since the GLRT-SIRV is only a GLRT with no guarantee of optimality. This phenomenon will be mathematically proved by the authors in a subsequent paper.

2.3 Robustness to signal mismatch

We question now the robustness of the GLRT-GAUSS and GLRT-SIRV detectors in the presence of signal mismatch. The received signal under hypothesis \mathcal{H}_1 is then $\mathbf{y} = A\mathbf{s}_b + \mathbf{n}$, where \mathbf{s}_b denotes the backscattered signal, while the test statistic will use signal \mathbf{s} . We assume that \mathbf{s}_b and \mathbf{s} differ by an angle $\alpha \in [0, \pi/2[$, i.e. the projection of \mathbf{s}_b onto the noise subspace $\overline{\Omega_S}$ is non zero, and: $\frac{|\mathbf{s}^H \Gamma^{-1} \mathbf{s}_b|^2}{\|\mathbf{s}\|_{\Gamma^{-1}}^2 \|\mathbf{s}_b\|_{\Gamma^{-1}}^2} = \cos^2 \alpha$.

A detector robust to signal mismatch should provide good performance detection at sufficiently large SNR even for distorted signals. We will therefore consider asymptotic performance of the GLRT-GAUSS and GLRT-SIRV detectors. Let us denote by $P_D^G(\rho, \alpha)$ and $P_D^S(\rho, \alpha)$ the detection

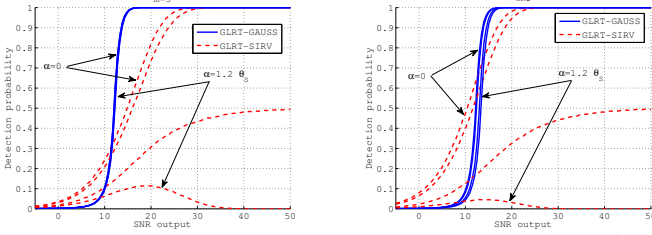


Figure 3: GLRT-GAUSS and GLRT-SIRV detection performance with signal mismatch of angles $\alpha = [0, \theta_S/2, \theta_S, \theta_S + \theta_S/5]$ and a K-distributed noise with shape parameter $\nu = 1$; $P_{FA} = 10^{-3}$, $m = 3$ (left) and $m = 5$ (right).

probabilities of the GLRT-GAUSS and GLRT-SIRV respectively for a given SNR ρ and a distortion angle α .

Theorem 1. (Robustness of the GLRT-GAUSS detector) For any distortion angle $0 \leq \alpha < \pi/2$, $\lim_{\rho \rightarrow +\infty} P_D^G(\rho, \alpha) = 1$.

Theorem 2. (Robustness of the GLRT-SIRV detector)

- For any $0 \leq \alpha < \theta_S$, $\lim_{\rho \rightarrow +\infty} P_D^S(\rho, \alpha) = 1$.
- For $\alpha = \theta_S$, $\lim_{\rho \rightarrow +\infty} P_D^S(\rho, \alpha) = 1/2$;
- For any $\theta_S < \alpha < \pi/2$, $\lim_{\rho \rightarrow +\infty} P_D^S(\rho, \alpha) = 0$.

Proofs of these theorems are provided in appendix A. They are illustrated by simulation results in Fig.3. They imply that the GLRT-GAUSS is robust, while the GLRT-SIRV may be dramatically affected by signal mismatch: the detector may even become completely inefficient if the distortion is large enough to cause the noiseless backscattered signal leave the decision cone. This effect is of course particularly harmful in low dimension when the decision cone is narrow.

3. HYBRID DETECTORS

The GLRT-SIRV detector is sensitive to the dimension and not robust to signal mismatch. However, as observed in Fig.2, it provides very good performance at low SNR for non-Gaussian noise. We propose here new detectors that provide similar performance at low SNR, and performance close to the GLRT-GAUSS at high SNR, with improved robustness and less sensitivity to the dimension.

3.1 Design of the decision region

The detectors we propose are built on a geometric heuristic. This may seem suboptimal but recall that the GLRT strategy is already an heuristic one. This geometric heuristic comes from the following comments: the GLRT-SIRV detector is performant at low SNR because its cone-shaped decision region permits to accept signals with low amplitudes if they are located near the signal subspace Ω_S . The GLRT-GAUSS is performant at high SNR and also robust because it accepts any signal gathering enough energy in the signal subspace.

The new hybrid detectors we propose are characterized by the shape of their acceptance region Φ_H , defined as

$$\Phi_H = \{ \mathbf{y} : \frac{|\mathbf{s}^H \mathbf{\Gamma}^{-1} \mathbf{y}|^2}{\|\mathbf{s}\|_{\mathbf{\Gamma}^{-1}}^2} > \tau_H \text{ OR } \frac{|\mathbf{s}^H \mathbf{\Gamma}^{-1} \mathbf{y}|^2}{\|\mathbf{s}\|_{\mathbf{\Gamma}^{-1}}^2 \|\mathbf{y}\|_{\mathbf{\Gamma}^{-1}}^2} > \cos^2 \theta_H \}.$$

The geometry of this decision region is represented in Fig.4. Φ_H depends on two parameters τ_H and θ_H that must be determined so as to ensure a given false alarm probability P_{FA} . θ_H can take any value in the interval $[0, \theta_S]$ where θ_S is the angle of the GLRT-SIRV decision cone for the P_{FA} considered; then, for a chosen value of θ_H , there is only one single value of τ_H that can ensure the desired P_{FA} . It verifies

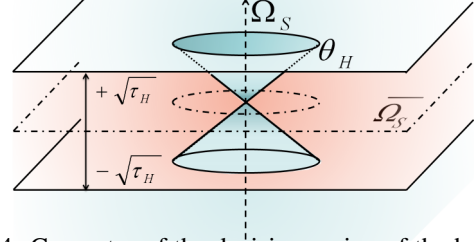


Figure 4: Geometry of the decision region of the hybrid detectors. Measurement falling outside the hyperplanes or in the cone (blue region) are accepted.

$\tau_H \geq \tau_G$. Any value of τ_H or θ_H outside their definition intervals would lead to false alarm probability larger than the desired P_{FA} . Limiting cases are $\tau_H = \tau_G$ for $\theta_H = 0$, and $\tau_H = +\infty$ for $\theta_H = \theta_G$. These two cases correspond to the GLRT-GAUSS and GLRT-SIRV detectors respectively. Note that the new detectors are not costly: they perform two tests similar to the GLRT-GAUSS and GLRT-SIRV tests, with a logical OR operation to merge the two results.

3.2 Performance of the hybrid detectors

3.2.1 Theoretical false alarm and detection probabilities

In this section, we provide theoretical expressions for the false alarm and detection probabilities of the proposed hybrid detector in Gaussian and SIRV noise. Since the hybrid detector is obtained by a logical OR operation between the GLRT-GAUSS and the GLRT-SIRV detector, it is clear that the false alarm and detection probabilities, denoted here by $P_{\mathcal{H}_0}^H(\tau_H, \theta_H)$ and $P_{\mathcal{H}_1}^H(\tau_H, \theta_H)$ respectively, are given by:

$$P_{\mathcal{H}_1}^H(\tau_H, \theta_H) = P_{\mathcal{H}_1, \kappa}^G(\tau_H) + P_{\mathcal{H}_1, \kappa}^S(\theta_H) - P_{\mathcal{H}_1, \kappa}^{AND}(\tau_H, \theta_H),$$

where $P_{\mathcal{H}_1, \kappa}^G(\tau_H)$, $P_{\mathcal{H}_1, \kappa}^S(\theta_H)$ and $P_{\mathcal{H}_1, \kappa}^{AND}(\tau_H, \theta_H)$ are respectively the probabilities under hypothesis \mathcal{H}_1 and random texture κ of the GLRT-GAUSS, the GLRT-SIRV and a detector obtained by a logical AND operation. Probabilities for the two first detectors are well known. We detail the computation for the probability of the last term in Appendix B, which can be expressed in SIRV noise as:

$$P_{\mathcal{H}_1}^{AND}(\tau_H, \theta_H) = \int_0^{+\infty} P_{\mathcal{H}_1}^G\left(\frac{\tau_H}{\kappa}\right) \int_0^{\frac{\eta_H}{\kappa}} p_{\chi_{2(m-1)}^2}(x_2) p_{\kappa}(\kappa) dx_2 d\kappa + \int_0^{+\infty} \int_{\frac{\eta_H}{\kappa}}^{+\infty} P_{\mathcal{H}_1}^G\left(\frac{x_2}{\tan^2 \theta_H} | x_2\right) p_{\chi_{2(m-1)}^2}(x_2) p_{\kappa}(\kappa) dx_2 d\kappa, \quad (4)$$

where $\eta_H = \tau_H \tan^2 \theta_H$, $p_{\chi_{2(m-1)}^2}(x)$ is the density probability of a central χ^2 random variable with $2(m-1)$ degrees of freedom, $P_{\mathcal{H}_1}^G$ is the false alarm or detection probability of the GLRT-GAUSS in Gaussian noise, and $p_{\kappa}(\kappa)$ is the density probability of the texture κ . Expressions for Gaussian noise can be simply obtained by setting $p_{\kappa}(\kappa) = \delta(\kappa - 1)$, in which case the integrals over the texture disappear.

3.2.2 Discussion

The particular design of the hybrid detectors, that uses information from both the signal energy and the signal angle, leads to very interesting performance: simulation results for several hybrid detectors corresponding to different decision angles θ_H are presented in Fig.5 for Gaussian and non-Gaussian noises. In Gaussian noise, hybrid detectors provide performance similar to the GLRT-GAUSS, thus greatly

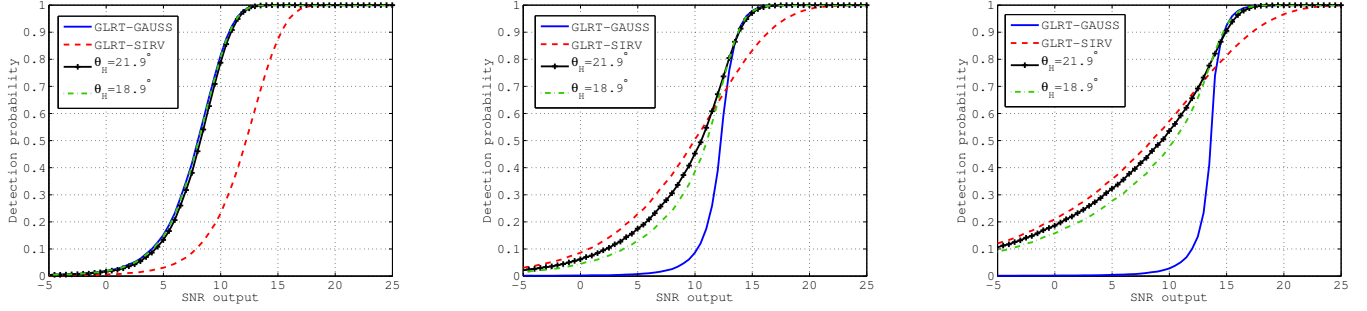


Figure 5: Hybrid detectors performance for different angles θ_H for: (left) Gaussian noise; (center) K-distributed noise with shape parameter $\nu = 1$; (right) K-distributed noise with shape parameter $\nu = 0.5$; $m = 5$, $P_{FA} = 10^{-3}$.

outperforming the GLRT-SIRV. In non-Gaussian noise, their performances are close to the GLRT-GAUSS at high SNR when this detector is the most performant. On the contrary, they provide performance better than the GLRT-GAUSS and very close to the GLRT-SIRV at low SNR when the latter is very performant. Note also that the detection performance of this detector is quite robust with respect to the choice of the decision angle θ_H .

3.2.3 Robustness to signal mismatch

We establish now the following robustness theorem, where $P_D^H(\rho, \alpha)$ represents the detection probability of the hybrid detector for a given SNR ρ and a distortion angle α :

Theorem 3. (Robustness of the hybrid detectors) For any distortion angle $0 \leq \alpha < \pi/2$ and any $0 \leq \theta_H < \theta_S$,

$$\lim_{A \rightarrow +\infty} P_D^H(\rho, \alpha) = 1.$$

This theorem states that, excepting for the particular case $\theta_H = \theta_S$, i.e. the GLRT-SIRV, the hybrid detectors are robust to signal mismatch. The proof is straightforward since these detectors behave asymptotically like the GLRT-GAUSS detector. The detection performance presented in Fig.6 validates this theorem. Interestingly, we see that when the mismatch is large, the hybrid detector tends to provide the same performance as the GLRT-GAUSS. Finally we highlight that the ASB detector from [8] can be proved to be robust only in a subset $[0, \theta_{ASB}]$ of $[0, \pi/2]$.

4. CONCLUSION

In this paper we have studied the GLRT-GAUSS and GLRT-SIRV detectors. We have presented their geometric properties, and analyzed their behavior with respect to dimension and signal mismatch. We have in particular stated that the GLRT-GAUSS detector is asymptotically robust to signal mismatch, whereas the GLRT-SIRV is asymptotically robust only in a reduced range of mismatch angles that depends on the detection threshold. We have then proposed a new family of detectors based on a geometric heuristic; it exploits good properties of both the GLRT-GAUSS and GLRT-SIRV. This family provides very good detection performance for Gaussian or non-Gaussian noise while being relatively insensitive to dimension. It can also be shown to be asymptotically robust to signal mismatch. The new geometric heuristic proposed here can be extended to continuous combinations that will design even more general families of detectors featuring any desired decision region.

A. PROOFS OF THEOREMS 1 AND 2

In all the proofs, we denote by $\mathcal{B}(c, r)$ the ball of center c and radius r , i.e. $\mathcal{B}(c, r) = \{\mathbf{x} \in \mathbb{C}^k : \|\mathbf{c} - \mathbf{x}\|^2 \leq r\}$. We will

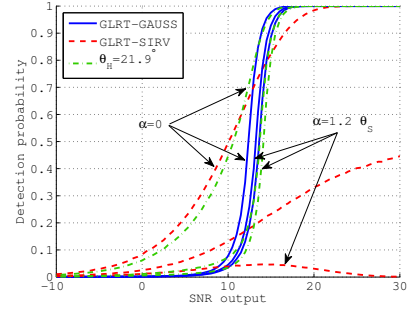


Figure 6: Hybrid detector performance for $\theta_H = 21.9^\circ$ in the presence of signal distortion of angle $\alpha = [0, \theta_S, \theta_S + \theta_S/5]$; $m = 5$, $P_{FA} = 10^{-3}$.

use the fact that for any probability density $p_{\mathbf{n}}(\mathbf{n})$, we have:

$$\forall 0 < p < 1, \exists M > 0 : \forall r \geq M, p \leq \int_{\mathcal{B}(\mathbf{0}, r)} p_{\mathbf{n}}(\mathbf{n}) d\mathbf{n} \leq 1. \quad (5)$$

Proof of Theorem 1. The idea of the proof is the following: we show that for any detection probability P_D and any distortion angle α , there exists an SNR value ρ for which we can design a region included in Φ_G of probability equal to P_D .

The received signal is given by $\mathbf{y} = A\mathbf{s}_b + \mathbf{n}$. We can assume for simplicity that $\|\mathbf{s}_b\|_{\Gamma^{-1}} = 1$ and $\sigma^2 = \mathbf{n}^H \Gamma^{-1} \mathbf{n}$. We then define the complex amplitude A such that $|A|^2 = \rho \sigma^2$, so that the SNR is equal to ρ . Let us denote finally $\mathbf{e}_s = \mathbf{s} / \|\mathbf{s}\|_{\Gamma^{-1}}$, that is the unit vector defining the signal space Ω_S . Using this notation, the GLRT-GAUSS decision region is $\Phi_G = \{\mathbf{y} : |y_1| \geq \sqrt{\tau_G}\}$ where $y_1 = \mathbf{e}_s^H \Gamma^{-1} \mathbf{y}$ is the projection of \mathbf{y} onto Ω_S . Let us also denote by $a_1 = A\mathbf{e}_s^H \Gamma^{-1} \mathbf{s}_b$ the projection of $A\mathbf{s}_b$ onto Ω_S . Then $|a_1| = |A| \cos \alpha$.

Now let $\varepsilon > 0$, and $p = 1 - \varepsilon$. Using (5), we can find M and a certain $r \geq M$ such that:

$$\int_{\mathcal{B}(A\mathbf{s}_b, r)} p_{\mathbf{y}}(\mathbf{y}) d\mathbf{y} = \int_{\mathcal{B}(\mathbf{0}, r)} p_{\mathbf{n}}(\mathbf{n}) d\mathbf{n} \geq p = 1 - \varepsilon. \quad (6)$$

We then choose an SNR value ρ such that $|A| \geq \frac{r + \sqrt{\tau_G}}{\cos \alpha}$; such a value exists for any $\alpha < \pi/2$. Then $|a_1| \geq r + \sqrt{\tau_G}$, and therefore, for all $\mathbf{x} \in \mathcal{B}(A\mathbf{s}_b, r)$, $|x_1| \geq \sqrt{\tau_G}$. Thus $\mathcal{B}(A\mathbf{s}_b, r) \subset \Phi_G$, and we have:

$$p \leq \int_{\mathcal{B}(A\mathbf{s}_b, r)} p_{\mathbf{y}}(\mathbf{y}) d\mathbf{y} \leq \int_{\Phi_G} p_{\mathbf{y}}(\mathbf{y}) d\mathbf{y} = P_D^G(\rho, \alpha) \leq 1.$$

Finally $\forall \varepsilon, \exists M > 0 : \forall r \geq M, 0 \leq 1 - P_D^G(\rho, \alpha) \leq \varepsilon$, and $\lim_{\rho \rightarrow +\infty} P_D^G(\rho, \alpha) = 1$ for any $\alpha < \pi/2$. \square

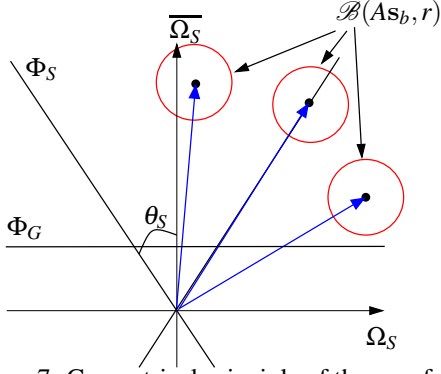


Figure 7: Geometrical principle of the proofs.

Proof of Theorem 2. Let us first consider the case $0 \leq \alpha < \theta_S$. Since the GLRT-SIRV decision region is a cone of angle θ_S , the distorted signal \mathbf{s}_b is contained in this cone. Again we can find M and a certain $r \geq M$ verifying (5). Moreover, the distance d between the vector \mathbf{As}_b and the surface of the cone is simply $d = |A| \sin(\theta_S - \alpha)$. Let us choose an SNR ρ such that $|A| \geq r / \sin(\theta_S - \alpha)$ (this is possible since we assume $0 \leq \alpha < \theta_S$). Then $d \geq r$, and therefore, for all $\mathbf{x} \in \mathcal{B}(\mathbf{As}_b, r)$, $\mathbf{x} \in \Phi_S$. Thus $\mathcal{B}(\mathbf{As}_b, r) \subset \Phi_S$, and we have:

$$p \leq \int_{\mathcal{B}(\mathbf{As}_b, r)} p_{\mathbf{y}}(\mathbf{y}) d\mathbf{y} \leq \int_{\Phi_S} p_{\mathbf{y}}(\mathbf{y}) d\mathbf{y} = P_D^S(\rho, \alpha) \leq 1.$$

Therefore $\forall \varepsilon, \exists M > 0 : \forall r \geq M, 0 \leq 1 - P_D^S(\rho, \alpha) \leq \varepsilon$, and $\lim_{\rho \rightarrow +\infty} P_D^S(\rho, \alpha) = 1$ for any $0 \leq \alpha < \theta_S$.

Let us now consider the case $\theta_S < \alpha < \pi/2$. We use the same reasoning, but this time we build a ball included in $\overline{\Phi_S}$. The distorted signal \mathbf{s}_b is now located outside the GLRT-SIRV cone. The distance d between vector \mathbf{As}_b and the surface of the cone is then $d = |A| \sin(\alpha - \theta_S)$. We choose $|A| \geq r / \sin(\alpha - \theta_S)$ (this is possible since we assume $\theta_S < \alpha < \pi/2$). Then similarly $\mathcal{B}(\mathbf{As}_b, r) \subset \overline{\Phi_S}$, and we have:

$$p \leq \int_{\mathcal{B}(\mathbf{As}_b, r)} p_{\mathbf{y}}(\mathbf{y}) d\mathbf{y} \leq \int_{\overline{\Phi_S}} p_{\mathbf{y}}(\mathbf{y}) d\mathbf{y} = 1 - P_D^S(\rho, \alpha).$$

Therefore $\forall \varepsilon, \exists M > 0 : \forall r \geq M, 0 \leq P_D^S(\rho, \alpha) \leq \varepsilon$, and $\lim_{\rho \rightarrow +\infty} P_D^S(\rho, \alpha) = 0$ for any $\theta_S < \alpha < \pi/2$.

Let us consider finally the particular case $\alpha = \theta_S$. For this case, a rigorous proof requires some technical developments that we will not display here. We will only explain briefly the idea: in this special case where \mathbf{As}_b exactly lies on the surface of the decision cone, we can prove that asymptotically (in terms of SNR), any ball $\mathcal{B}(\mathbf{As}_b, r)$ will be exactly splitted into two equal halves by the decision cone, thus leading to a detection probability of $1/2$. \square

B. P_{FA} AND P_D COMPUTATION

Let us denote by y_1 and y_2 the squared norms of the projection of \mathbf{y} onto Ω_S and $\overline{\Omega_S}$ respectively. The GLRT-GAUSS and GLRT-SIRV test statistics can be expressed as

$$\mathcal{T}_G = y_1 \quad \text{and} \quad \mathcal{T}_S = \frac{y_1}{y_1 + y_2}, \quad \text{and thus:}$$

$$\begin{aligned} P_{\mathcal{H}_i}^{AND}(\tau_H, \theta_H) &= Pr(y_1 > \tau_H \text{ AND } y_1 > \frac{y_2}{\tan^2 \theta_H} | \mathcal{H}_i) \\ &= Pr(y_1 > \max\left(\tau_H, \frac{y_2}{\tan^2 \theta_H}\right) | \mathcal{H}_i). \end{aligned}$$

From the SIRV model, we can write $y_1 = \kappa x_1$ and $y_2 = \kappa x_2$ where κ is the texture. Then, x_1 is a central (under \mathcal{H}_0) or non central (under \mathcal{H}_1) χ^2 random variable with 2 degrees of freedom, while x_2 is a central χ^2 random variable with $2(m-1)$ degrees of freedom under both hypotheses \mathcal{H}_0 and \mathcal{H}_1 . Conditioning the previous expression on κ , we get:

$$P_{\mathcal{H}_i}^{AND} = \int_0^{+\infty} Pr(x_1 > \max\left(\frac{\tau_H}{\kappa}, \frac{x_2}{\tan^2 \theta_H}\right) | \mathcal{H}_i, \kappa) p(\kappa) d\kappa$$

$$\text{Since } \max\left(\frac{\tau_H}{\kappa}, \frac{x_2}{\tan^2 \theta_H}\right) = \begin{cases} \frac{\tau_H}{\kappa} & \text{if } x_2 \leq \frac{\tau_H \tan^2 \theta_H}{\kappa}, \\ \frac{x_2}{\tan^2 \theta_H} & \text{otherwise,} \end{cases}$$

the precedent expression can be conditioned on x_2 and splitted into two parts as:

$$\begin{aligned} P_{\mathcal{H}_i}^{AND} &= \int_0^{+\infty} \int_0^{\frac{\eta_H}{\kappa}} Pr(x_1 > \frac{\tau_H}{\kappa} | \mathcal{H}_i) p(x_2) p(\kappa) dx_2 d\kappa \\ &+ \int_0^{+\infty} \int_{\frac{\eta_H}{\kappa}}^{+\infty} Pr(x_1 > \frac{x_2}{\tan^2 \theta_H} | \mathcal{H}_i) p(x_2) p(\kappa) dx_2 d\kappa, \end{aligned}$$

where $Pr(x_1 > s | \mathcal{H}_i)$ is the false alarm or detection probability of the GLRT-GAUSS in Gaussian noise, which is provided by a central (under \mathcal{H}_0) or non central (under \mathcal{H}_1) χ^2 density with 2 degrees of freedom. The final expression (4) follows.

REFERENCES

- [1] V. Anastassopoulos, G. Lampropoulos, A. Drosopoulos, and M. Rey. High resolution radar clutter statistics. *IEEE Trans. Aero. and Elec. Sys.*, 35(1):43–60, 1999.
- [2] J. Billingsley, A. Farina, F. Gini, M. Greco, and L. Verrazzani. Statistical analyses of measured radar ground clutter data. *IEEE Trans. Aero. and Elec. Sys.*, 35(2):579–593, 1999.
- [3] E. Conte, M. Lops, and G. Ricci. Asymptotically Optimum Radar Detection in Compound-Gaussian Clutter. *IEEE Trans. Aero. and Elec. Sys.*, 31(2):617–625, 1995.
- [4] A. De Maio, S. De Nicola, and A. Farina. GLRT Versus MFLRT for Adaptive CFAR Radar Detector With Conic Uncertainty. *IEEE Sig. Proc. Lett.*, 16(8):707–710, 2009.
- [5] A. De Maio, S. De Nicola, Y. Huang, S. Zhang, and A. Farina. Adaptive Detection and Estimation in the Presence of Useful Signal and Interference Mismatches. *IEEE Trans. Sig. Proc.*, 57(2):436–450, 2009.
- [6] E. Jay, J.-P. Ovarlez, D. Declercq, and P. Duvaut. BORD: Bayesian optimum radar detector. *Signal Processing*, 83:1151–1162, 2003.
- [7] S. Kay. *Fundamentals of Statistical Signal Processing. Detection theory*. Prentice Hall, 1998.
- [8] C. Richmond. Performance of the Adaptive Sidelobe Blanker Detection Algorithm in Homogeneous Environments. *IEEE Trans. Sig. Proc.*, 48(5):1235–1247, 2000.
- [9] L. Scharf and B. Friedlander. Matched Subspace Detectors. *IEEE Trans. Sig. Proc.*, 42(8):2146–2157, 1994.
- [10] K. Yao. A Representation Theorem and Its Applications to Spherically-Invariant Random Processes. *IEEE Trans. Inf. Theo.*, 19(5):600–608, 1973.